https://doi.org/10.5194/esurf-2021-97
Preprint. Discussion started: 20 December 2021

Earth Surface Dynamics Discussions
Open Access
EGU

Regularity of transportation for cohesive bank-collapsed materials

Guosheng Duan[1, 3], Haifei Liu [2, 3, *]
[1]Faculty of Geographical Science, Beijing Normal University, Beijing 100875, China.
[2]Key Laboratory of Hydro-Sediment Science and River Training, the Ministry of Water Resources, China Institute of Water Resources and Hydropower Research, Beijing 100048, China.
[3]School of Environment, Key Laboratory of Water and Sediment Sciences of MOE, Beijing Normal University, Beijing 100875, China.
* Correspondence: haifei.liu@bnu.edu.cn

Abstract: The transportation of bank-collapsed materials is a key issue among river evolution processes. In this study, a series of flume experiments were conducted to monitor riverbank collapse processes and to explore the regularity of transportation for cohesive collapsed materials. The collapsed materials, both the bed and suspended loads, that transformed from collapsed materials were intensively evaluated under experimental conditions. The results showed that the collapsed materials contributed to 12 ~ 20% sedimentation in situ, 8 ~ 14% suspended loads and 70 ~ 80% bed loads. In addition, the bed load motion efficiency coefficient (e_b), suspended load motion efficiency coefficient (e_s) and sediment carrying capacity factor ($U^3/gR\omega$) were introduced to describe the transportation of collapsed materials in terms of energy dissipation. This research provides theoretical and practical benefits for predicting channel evolution processes.

Keywords: riverbank, collapsed materials, transformation, cohesive

1. Introduction

Riverbank collapse, which occurs in alluvial streams worldwide, has caused a series of social, economic and environmental problems (Simon et al., 2009, Rinaldi and Nardi, 2013, Hackney et al., 2015). Moreover, collapsed materials are also a major stream sediment source, directly influencing sediment concentration and riverbed evolution processes in both local and downstream areas (Motta et al., 2014). Thus, more research has concentrated on the mechanisms and channel evolution processes associated with riverbank collapse in recent years (Patsinghasanee et al., 2017; Arai et al., 2018; Deng et al., 2019; Lopez & Lanzoni, 2019; Masoodi et al., 2019; Yu et al., 2020; Zhao et al., 2020).

https://doi.org/10.5194/esurf-2021-97
Preprint. Discussion started: 20 December 2021

Riverbank collapse processes are usually decomposed into two steps: bank toe erosion and upper riverbank failure (Thorne & Tovey, 1981; Lawler et al., 1997; Simon et al., 2000). For cohesive riverbanks, bank toe erosion occurred through entrainment of aggregates because of the electrochemical forces existing among the fine particles (Wood et al., 2001; Langendoen & Simon,2008). The collapse patterns can be classified as plane, arch and cantilever collapse based on the shape of the collapse plane (Darby et al., 2000). The roles of various influencing factors, mainly vegetation (Simon & Collison., 2002; Yu et al., 2020), soil properties (Parker et al., 2008; Masoodi et al., 2017), bank shape (Baker, 1981; Simon & Rinaldi, 2006), hydraulic conditions (Visconti et al., 2010; Chiang et al., 2011; Chen et al.,2017) and underground water level (Casagli et al., 1999; Dapporto et al., 2001; Rinaldi et al., 2004), were also evaluated in detail in riverbank collapse processes. Based on these achievements, several bank erosion models were set up to predict cohesive riverbank collapse, of which the bank toe erosion rate was obtained by the difference between flow shear stress and soil shear strength, while riverbank stability was estimated by a stability coefficient (F_s) of the ratio of driving force to resistance (Hook, 1980; Osman & Thorne, 1988; Simon et al., 2009; Clark & Wynn, 2007). As the models took into accounting the influencing factors, they were widely used to quantify riverbank collapse and simulate the channel evolution process in collapsed reaches.

Many researchers have combined bank erosion models with water-sediment mathematical models to simulate channel evolution processes (Nagata et al., 2000; Darby et al., 2002; Chen & Duan, 2006; Rinaldi et al., 2008; 2013; Xu et al., 2011; Motta et al., 2012). It is known that some collapsed materials were transported by flow current instantaneously after the riverbank collapsed, while others accumulated at the bank toe. Evaluating the deposition and further movement of the accumulated materials remains a key problem to be solved. In previous simulations, various assumptions were established: (1) collapsed materials were transported immediately by the water current (Darby et al., 2007; Rinaldi et al., 2008); (2) 50% of the collapsed materials accumulated at bank toe and then participated in riverbed evolution process (Xia et al., 2016; Deng et al., 2019); (3) collapsed material particles that are coarser than 0.062 mm would distribute uniformly across the bed area between bank toe and the boundary of the near-bank sediment routing segment, from a distance equal to two bank heights (Rijn and Leo, 1985); (4) the volume of collapsed materials accumulated at bank toe was decided by sediment carrying capacity which equals the maximal sediment

https://doi.org/10.5194/esurf-2021-97
Preprint. Discussion started: 20 December 2021

concentration for nonequilibrium transportation of the suspended load (Jia et al., 2010; Duan et al., 2018; Shu et al., 2019). Although a number of relatively accurate simulation results were obtained based on these assumptions, there has been no direct evidence to expound the distribution and transportation of collapsed materials in detail. Certain advantages have been provided through water flume experiments, such as the distribution of cohesive collapsed materials along noncohesive riverbeds, the mixture of collapsed and bed sediments, and the relationship between sediment distribution and velocities (Yu et al., 2013; 2014; 2016). These results mainly focused on qualitatively describing the phenomenon. However, the quantity of sediment transportation was not involved, especially in collapsed materials. Thus, one object of this study is to quantify the transportation of collapsed materials, which is a key issue when predicting the riverbed evolution process.

In addition, collapsed materials that accumulate at the bank toe will initiate first and then transform into bed and suspended load in the following river evolution processes. From the point of energy dissipation, the energy of bed load motion comes from water potential energy, while sediment suspension energy comes from the turbulent kinetic energy of water flow (Huang et al., 2005). The transportation of accumulated sediments depends not only on the relationship between sediment gravity and current shear stress but also on the ratio between the energy expended in motion and the water potential energy available (Qian & Wan, 1983). To describe the transportation of collapsed materials in detail, the energy dissipation of sediment transportation was investigated in this study.

Overall, a series of flume experiments were conducted to simulate cohesive riverbank collapse processes and characterize the transportation of collapsed materials. The major objectives of this study are as follows: (1) to quantify the sediment transformation due to riverbank collapse, especially the collapsed materials transforming into bed and suspended loads, and (2) to analyze the transportation of collapsed materials in terms of energy dissipation.

2. Experimental Methods

2.1 Experimental setup and materials

Experiments were performed in a 25 m long rectangular flume with a width and depth of 0.8 m (Figure 1), located at the Key Laboratory of Water and Sediment Science

https://doi.org/10.5194/esurf-2021-97
Preprint. Discussion started: 20 December 2021

Earth Surface Dynamics Discussions
Open Access

of MOE (Ministry of Education), Beijing Normal University, China. The experiments consisted of four groups with different bank slopes (45°, 60°, 75°, 90°). For each group, a 2.4 m long, 0.15 m deep symmetric trapezoidal channel with a 0.4 m bottom width was built within the flume, while the width of the channel top was determined by bank slopes, as listed in Table 1. Riverbanks of both sides were made of the selected materials collected from a natural bank at the Dengkou reach of the Yellow River (Shu et al., 2019). The gravel was laid up and downstream of the recreated banks to enable constant boundary conditions (Figure 1). Five typical sections (S1-S5) were also set up at 40 cm intervals to monitor the relevant parameters, and three measuring lines were set in each section to monitor the velocities (Figure 1). Multiple locations within measuring lines of typical sections were selected to ensure the accuracy of velocities by using a propeller (Figure 2). Figure 3 shows the top view of the actual experimental setup, with water level gauges and pore-water pressure gauges fitted in the flume to monitor the water level and pore water pressure, respectively.

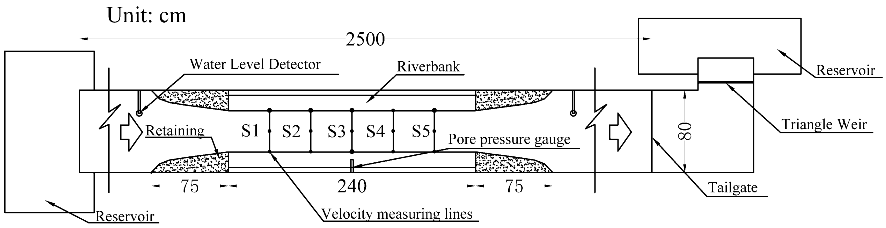

Figure 1. Schematic diagram of the test flume (not to scale) (Unit: cm).

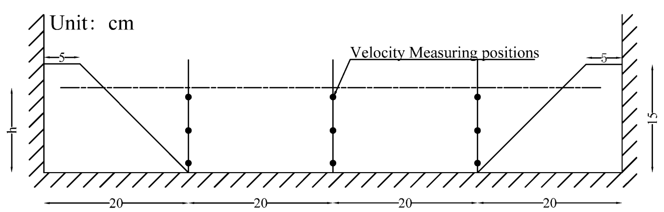

Figure 2. Example of one cross section and corresponding monitoring positions for the velocity.

Before each experiment, the particle size distribution (Figure 4) and physical properties of experimental materials taken from typical sections were tested. At the preparatory stage, the tailgate was kept closed, and the water level rose slowly to the designed level. Then, the initiation of experiment began by adjusting the designed flow conditions (Table 1). Water samples containing materials were taken every three minutes at Sections S1, S3, S5 and at the tailgate to measure the sediment concentration.

https://doi.org/10.5194/esurf-2021-97
Preprint. Discussion started: 20 December 2021

The experiment was considered completed when no more riverbank materials were removed or eroded.

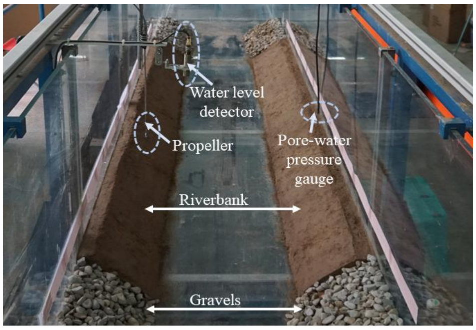

Figure 3. Actual experimental setup with bank slope 45°.

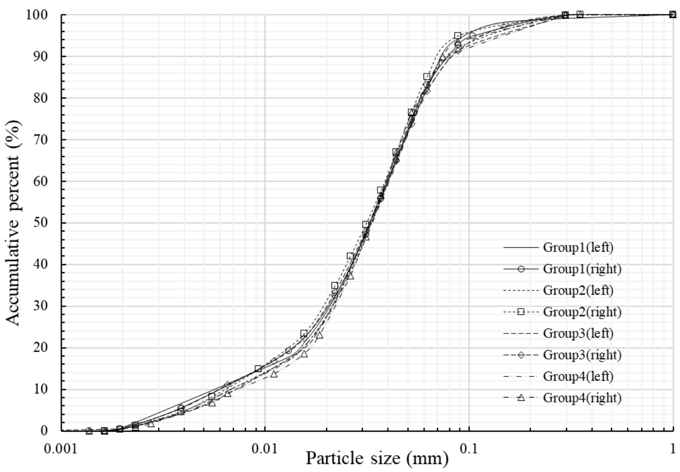

Figure 4. Particle size distribution of the materials.

Table 1. Configurations and bank morphology details.

Group	Slope degree (°)	Bank morphology (left and right)			Flux (L/s)	Water discharge time (min)	Water level (cm)
		Bank top width (cm)	Bank height (cm)	Bank toe width (cm)			
No.1	45	5	15	20	38	30	11.5
					44	30	12.7
No.2	60	11.35	15	20	29.4	30	11
					40.9	30	12.75
No.3	75	16	15	20	27.8	30	10
					36.5	30	13.15
No.4	90	20	15	20	26	30	9.25
					33.8	30	12

https://doi.org/10.5194/esurf-2021-97
Preprint. Discussion started: 20 December 2021

3. Results and Discussion

3.1 Results

3.1.1 Quantity of sediment transportation due to riverbank collapse

After collapsed materials entered the channel, the incipient sediments were then further activated and transported as bed and suspended loads, while the remaining sediments accumulated at the toe of the bank. In summary, collapsed materials will be transported in three patterns: accumulated sand, bed loads and suspended loads.

(1) Quantity of collapsed materials

The amount of collapsed materials was obtained by comparing the topography of the riverbank before and after the experiment. Ten sections (C1, C2,···, C10) among riverbanks with 20 cm intervals along the flow direction were selected to measure the riverbank shape by using a glass plate with gridlines (Figure 5). Figure 8 shows the collapsed areas of the selected sections with a riverbank slope of 45°. Based on the unit weight of materials listed in Table 2, the quantities of the collapsed materials can be obtained in Table 3.

Table 2. Physical properties of the material tested for each configuration.

Group	Soil position	Moisture content (%)	Unit weight (g/cm^3)	Cohesion (kPa)	Friction angle (°)
No.1	Left bank	16.11	1.63	14.77	19.46
	Right bank	16.51	1.85	14.45	19.19
No.2	Left bank	16.01	1.81	14.77	19.46
	Right bank	16.18	1.77	14.45	19.19
No.3	Left bank	16.86	1.81	13.66	18.54
	Right bank	16.39	1.83	12.93	17.92
No.4	Left bank	17.42	1.81	13.77	18.63
	Right bank	18.04	1.68	15.37	19.96

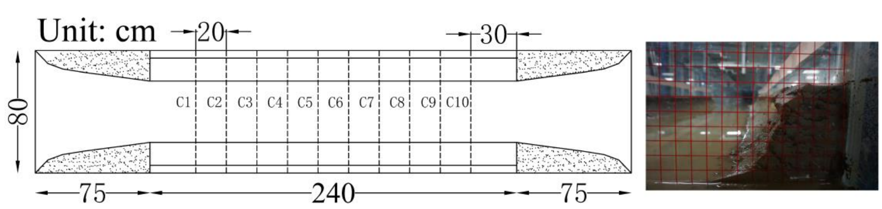

https://doi.org/10.5194/esurf-2021-97
Preprint. Discussion started: 20 December 2021

Figure 5. The measurement of riverbank shape by using a glass plate with gridlines.

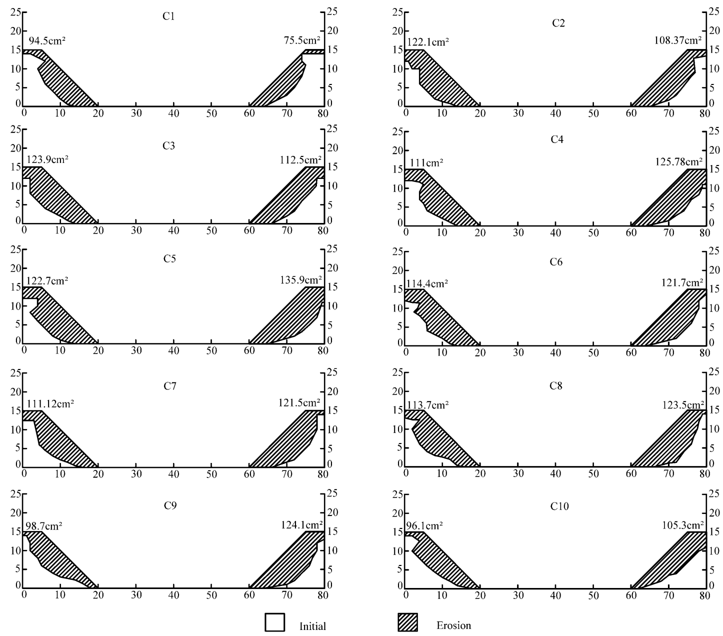

Figure 6. Collapsed areas of selected sections with riverbank slope 45°.

Table 3. Quantity of collapsed materials.

Group	Slope gradient (°)	Collapse amount (kg)
No.1	45	87.16
No.2	60	41.58
No.3	75	62.45
No.4	90	82.43

(2) Quantity of collapsed sediments accumulated at the toe of the bank

It is generally believed that the collapsed materials entering the channel can be treated as single-particle sediments, and the incipient motion particle size was calculated by the following equation (Qian and Wan, 1983):

$$\frac{U_i}{\sqrt{gD}} = \sqrt{\frac{\gamma_s - \gamma}{\gamma}\left(6.25 + 41.6\frac{h}{Ha}\right) + \left(111 + 740\frac{h}{Ha}\right)\frac{Ha\delta_0}{D^2}} \quad (1)$$

where Ha is the atmospheric pressure expressed in terms of water column height, Ha = 10 m; δ_0 is the thickness of a water molecule, $\delta_0 = 3.0 \times 10^{-8}$ cm; γ_s is the unit weight of sediment, γ_s = 17542 Nm^{-3}; γ is the unit weight of water, γ = 9800 Nm^{-3}; g is the gravitational acceleration, g = 9.8 ms^{-2}; D is the sediment particle size, m; U_i is the

https://doi.org/10.5194/esurf-2021-97
Preprint. Discussion started: 20 December 2021

velocity for incipient sediment motion, ms^{-1}; U is the velocity, ms^{-1} (for this study $U_i = U$), and h is the water depth, m.

Table 4 presents the percentage of accumulated sediments under different experimental conditions. It should be noted that particles between the lower and upper limits of incipient motion particle size could be incipient, whereas others were regarded as the accumulated sediments.

Table 4. Percentage of accumulated sediments under different experimental conditions.

Group	Slope gradient (°)	Flow discharge (L/s)	Average water level (cm)	Average flow rate (m/s)	Incipience motion particle size (lower limits) (μm)	Incipience motion particle size (upper limits) (mm)	Incipience motion percentage (%)	Accumulated sediment percentage (%)
No.1	45	38.00	11.50	0.61	9.48	3.40	88.06	11.94
		44.00	12.70	0.71	9.28	3.46	91.06	8.94
No.2	60	29.40	11.00	0.51	15.00	2.36	79.81	20.19
		40.90	12.75	0.59	10.40	3.12	82.91	17.09
No.3	75	27.80	10.00	0.57	11.00	3.03	85.56	14.44
		36.50	11.75	0.65	8.30	3.89	86.96	13.04
No.4	90	26.00	9.25	0.54	12.00	2.73	84.48	15.52
		33.80	12.00	0.59	10.19	3.17	87.24	12.76

(3) Quantity of bed and suspended loads transformed from collapsed materials

Table 5. The critical particle size of the collapsed riverbank.

Group	Bank slope (°)	Flow rate (L/s)	Critical particle size (mm)
No.1	45	38	0.018
		44	0.016
No.2	60	29.4	0.020
		40.9	0.018
No.3	75	27.8	0.018
		36.5	0.016
No.4	90	26	0.018
		33.8	0.016

In sediment-laden flow, coarse particles are usually transported as bed loads, while fine particles are transported as suspended loads. Although there were mutual transformations between these two in the transport processes, the quantities of bed and suspended loads transported by the water flow remained roughly the same under certain flow conditions. Thus, a critical particle size was introduced to divide the bed and suspended loads, with particles larger than the critical particle size were arranged as bed loads; otherwise, they were arranged as suspended loads. The method described in

https://doi.org/10.5194/esurf-2021-97
Preprint. Discussion started: 20 December 2021

detail in the literature (Shu et al., 2019) was adopted to obtain the critical particle size, as shown in Table 5.

Based on the bank material particle size distribution in Figure 4, the percentage of bed and suspended loads for each group can be obtained (Table 6).

Table 6. Mass percentage of sediment fractions.

Group	Bank slope (°)	Flow rate (L/s)	Incipient motion percentage (%)	Suspended load percentage (%)	Bed load percentage (%)
No.1	45	38	11.94	13.56	74.50
		44	8.94	15.26	75.80
No.2	60	29.4	20.19	7.88	71.93
		40.9	17.09	13.25	69.66
No.3	75	27.8	14.44	10.56	75
		36.5	13.04	11.3	75.66
No.4	90	26	15.52	9.39	75.09
		33.8	12.76	7.94	79.30

3.1.2 The transportation of collapsed materials in terms of energy dissipation

In this study, the bed load motion efficiency coefficient (e_b) and suspended load motion efficiency coefficient (e_s) were applied to describe the transportation of collapsed materials. Based on previous studies, e_b represents the transformation efficiency from the water potential energy into bedload motion (Bagnold, 1966), while e_s represents the transformation efficiency from turbulent kinetic energy into suspended load motion (Shu et al., 2007). The sediment carrying capacity equation can be expressed as the following (Qian & Wan, 1983):

$$S_*=k\left(U^3/gR\omega\right)^m ,$$

where S_* is the sediment carrying capacity, m^3s^{-1}; k and m are parameters; U is the velocity, ms^{-1}; g is the gravitational acceleration, ms^{-2}; R is the hydraulic radius, m; and ω is the sediment settling velocity, m/s. The sediment carrying capacity factor ($U^3g^{-1}R^{-1}\omega^{-1}$) can be regarded as the ratio of $U^2g^{-1}R^{-1}$ to ωU^{-1}, which represents the turbulence intensity and action of effective gravity, respectively. For these three parameters containing all kinds of energy factors, it is reasonable to study the transportation of the collapsed materials by building the relationship between e_b and $U^3g^{-1}R^{-1}\omega^{-1}$ and between e_s and $U^3g^{-1}R^{-1}\omega^{-1}$. The experimental data used were collected at two-minute intervals in Section S3 after riverbank collapse occurred.

https://doi.org/10.5194/esurf-2021-97
Preprint. Discussion started: 20 December 2021

(1) The relationship between e_b and $U^3g^{-1}R^{-1}\omega^{-1}$

The bedload motion efficiency coefficient (e_b) can be obtained by the following equations (Bagnold, 1966):

$$e_b = \left(u_* - u_{*c}\right)\left\{1 - \left[5.75u_* \lg\left(0.4h/mD\right) + \omega\right]/U_L\right\}/u_* \tag{2}$$

$$m = K\left(\frac{u_*}{u_{*c}}\right)^{0.6} \tag{3}$$

$$\omega = \left[\left(13.95\upsilon/D\right)^2 + 1.09(\gamma_s - \gamma)gD/\gamma\right]^{1/2} - 13.95\upsilon/D \tag{4}$$

$$u_* = \sqrt{gRJ} \tag{5}$$

$$u_{*c} = \left(\tau_c/\rho\right)^{1/2} \tag{6}$$

where u_* is frictional velocity, ms^{-1}; U_L is mean vertical velocity at the location of 0.4 h, m/s; h is the water depth, m; D is grain diameter, m; K is a constant coefficient (K=1.4 ~ 2.8); u_{*c} is critical shear velocity, m/s; γ_s is sediment unit weight, Nm^{-3}; γ is water unit weight, Nm^{-3}; ν is motion viscous coefficient, m^2s^{-1}, and $\nu = 1.31\times10^{-6}\ m^2s^{-1}$; J is hydraulic gradient; τ_c is flow shear stress, Nm^{-2}; and ρ is water density, kgm^{-3}.

The relationships between e_b and $U^3g^{-1}R^{-1}\omega^{-1}$ for different groups are shown in Figure 7.

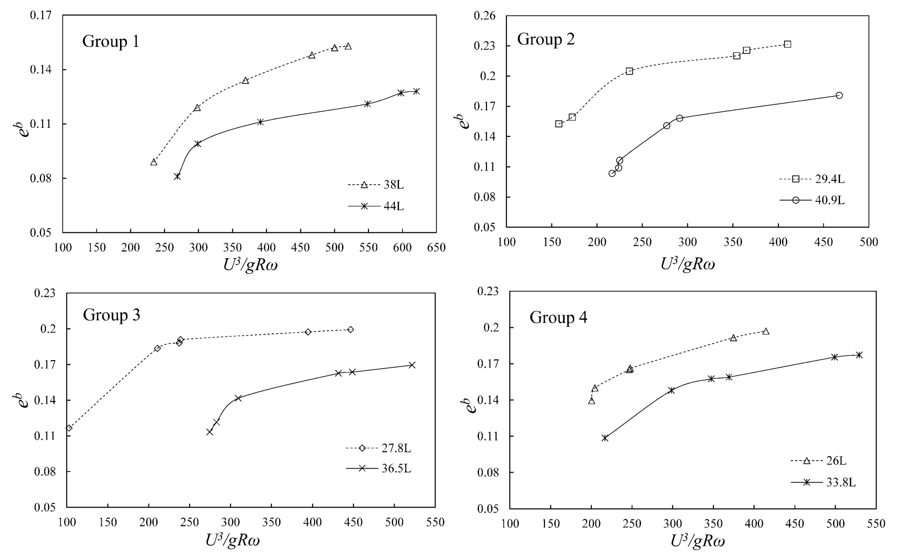

Figure 7. Relationship between e^b and $U^3/gR\omega$.

The range of e_b was 0.11 ~ 0.25, which was similar to Bagnold's result of 0.11 ~ 0.15, and e_b had a noticeable positive correlation relationship with $U^3g^{-1}R^{-1}\omega^{-1}$ (Bagnold, 1966). For each curve, e_b first quickly increased and then stabilized because after the

https://doi.org/10.5194/esurf-2021-97
Preprint. Discussion started: 20 December 2021

riverbank collapsed, the collapsed materials first accumulated at the toe of the bank and then transformed into bed loads. With increasing sediment carrying capacity, the energy of bed load motion increases. While the river gradually transferred from the nonequilibrium state to the equilibrium state, e_b tended to be stable.

In each group, the e_b value of the lower flow was larger than that of the higher flow, because as the flow increased, a portion of the bed load would transform into suspended load. Additionally, part of the energy for the bed load motion would convert into the particles' potential energy with the change of particles' position.

(2) The relationship between e^s and $U^3g^{-1}R^{-1}\omega^{-1}$

The suspended load motion efficiency coefficient (e_s) can be obtained by the following (Shu et al., 2008):

$$e_s = p \cdot \frac{\left[\lg\left(\mu_r + 0.1\right)\right]^N}{\kappa^2 k_t}\left(\frac{f_m}{8}\right)^{\frac{1}{2}} \cdot \left[\frac{1}{\kappa^2}\left(\frac{f_m}{8}\right)^{\frac{3}{2}} \frac{\gamma_m}{\gamma_s - \gamma_m}\frac{U^3}{gR\omega}\right]^{N-1} \quad (7)$$

$$k_t = 1 - 2\mu_r k_d U / \tau_c h \quad (8)$$

$$f_m = 0.11a\left(\frac{k_s}{4R} + \frac{68}{R_{em}}\right)^{0.25} \quad (9)$$

$$R_{em} = \frac{u_* D}{\upsilon} = \frac{\sqrt{ghJ}\,D}{\upsilon} \quad (10)$$

where μ_r is the relative dynamic viscosity coefficient, $\mu_r = 1+2.5S_v$; S_v is the volume sediment content; κ is the Karman constant, κ=0.4, p=0.3551, N=0.72, k_t is the turbulent kinetic energy conversion efficiency; k_dU is the vertical maximum velocity, m/s; f_m is the drag coefficient of sediment laden flow; α is the reduced drag coefficient, which is smaller than 1; k_s is the riverbed roughness coefficient, k_s=2D; and R_{em} is the muddy water Reynolds number.

https://doi.org/10.5194/esurf-2021-97
Preprint. Discussion started: 20 December 2021

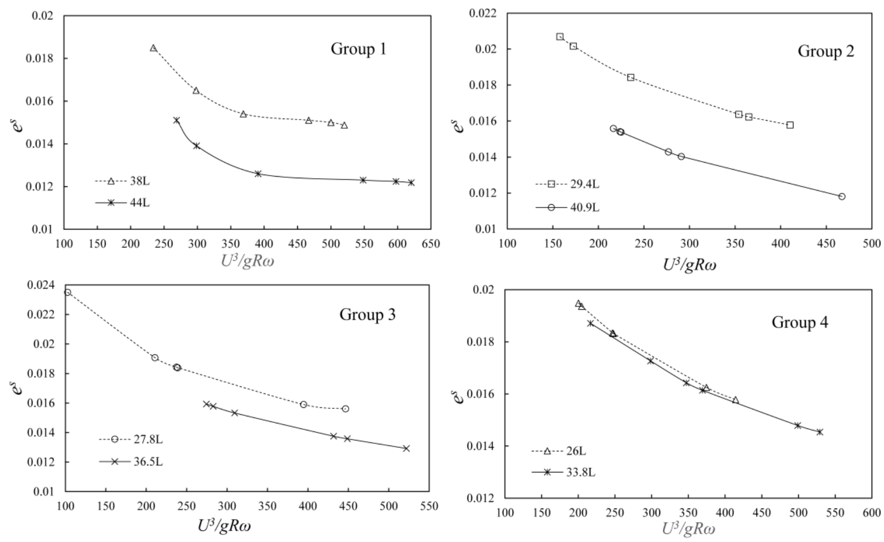

Figure 8. Relationship between e^s and $U^3/gR\omega$.

The range of e_s is 0.0129 ~ 0.0235, which was slightly different from Bagnold's result of 0.023 ~ 0.046 (Bagnold, 1966), but the values were still in the range of 0.00004−0.20 presented by Qian & Wan (1965). For each curve, e_s had a noticeably negative correlation relationship with $U^3g^{-1}R^{-1}\omega^{-1}$. After the riverbank collapsed, the river would transfer from a nonequilibrium state to equilibrium, and the suspended load concentration would increase compared with that of the noncollapse. However, sediment suspension energy decreased because of the drag reduction of suspended sediments provided by Zhang (1963). Moreover, in each group, e_s of the lower flow charge is larger than that of the higher flow, as when the flow charge increased, more bed loads would transform into suspended loads, with the drag reduction of suspended sediments (e_s decreased).

3.2 Discussion

In this study, riverbanks were built on both sides of the water flume, which was different from previous correlated studies (Yu et al., 2013; Shu et al., 2019; Zhao et al., 2020). The similar channel shape and on-site materials made this study more scientific for monitoring riverbank collapse processes. The quantities of the collapsed materials, bed and suspended loads obtained by the critical particle size method presented a good reference to predict the channel evolution process. The bed load motion efficiency coefficient (e_b), suspended load motion efficiency coefficient (e_s) and sediment carrying

https://doi.org/10.5194/esurf-2021-97
Preprint. Discussion started: 20 December 2021

capacity factor ($U^3g^{-1}R^{-1}\omega^{-1}$) were used to describe the transportation of collapsed materials, which differed from previous literature. Thus, this study can be considered a valuable attempt to scientifically describe the transportation of collapsed materials.

There are still limitations that need to be addressed within future research. First, the quantity of the collapsed materials, bed and suspended loads in this study were obtained under specific flow conditions. For the complicacy of natural rivers, more bank shapes, angles and flow conditions should be considered. Second, although the law of energy dissipation is a promising approach to describe the transportation of collapsed materials, studies of sediment transportation in terms of energy dissipation are usually qualitative. More accurate measurement tools need to be explored and applied to obtain the energy consumed by the bed and suspended loads. Finally, both quantities and energy dissipation should be studied comprehensively to analyze the transportation of collapsed materials and benefit channel evolution prediction.

4. Conclusions

A series of experiments with a constructed riverbank on both sides were conducted to quantify the transportation of the collapsed materials. Transportation was also studied from the point of energy dissipation. The findings can be concluded as follows:

(1) After the riverbank collapsed, the three main processes of the collapsed materials were deposited on-site and transported as bed and suspended load. In terms of the quantities, the percentages of these three were 12 ~ 20%, 70 ~ 80% and 8 ~ 14%, respectively.

(2) In the transportation of the collapsed materials, the ranges of e_b and e_s were 0.11 ~ 0.25 and 0.0129 ~ 0.0235, respectively. The drag reduction of the suspended loads was verified by the relationships between e_b, e_s and $U^3g^{-1}R^{-1}\omega^{-1}$.

(3) In terms of energy dissipation, the transportation of collapsed materials follows the law of river transition from a nonequilibrium to an equilibrium state. After the riverbank collapsed, the collapsed materials first transformed into bed loads. With the increase in the sediment carrying factor ($U^3g^{-1}R^{-1}\omega^{-1}$) toward the river equilibrium state, more bed load sediment transformed into suspended loads. At the same time, part of the energy for bed load motion would convert into the particles' potential energy.

The results can help reveal the mechanisms of channel bend evolution and provide valuable theoretical and practical benefits to river channel embankments.

Data availability

All raw data can be provided by the corresponding authors upon request.

Author contributions

GD performed the measurements and wrote the manuscript draft; HL reviewed and edited the manuscript.

Competing interests

The authors declare that they have no conflict of interest.

Acknowledgments

This work is supported by the Open Research Fund of Key Laboratory of Hydro-Sediment Science and River Training, the Ministry of Water Resources, China Institute of Water Resources and Hydropower Research [Grant number: IWHR-JH-2020-A-03] and the National Natural Science Foundation of China [Grant number: 51779011].

Financial support

This work is supported by the Open Research Fund of Key Laboratory of Hydro-Sediment Science and River Training, the Ministry of Water Resources, China Institute of Water Resources and Hydropower Research [Grant number: IWHR-JH-2020-A-03] and the National Natural Science Foundation of China [Grant number: 51779011].

References

Arai, R., Ota, K., Sato, T., and Toyoda, Y.: Experimental investigation on cohesionless sandy bank failure resulting from water level rising. Int. J. Sediment Res., 33, 47-56, https://doi.org/10.1016/j.ijsrc.2017.08.002, 2018.

Bagnold, R. A.: An approach to the sediment transport problem from general physics. US Geolo. Sur. Prof., 422, 1-37, https://doi.org/10.1017/S0016756800049074, 1966.

Baker, R. (1981). Tensile strength, tension cracks, and stability of slopes. Soils Found., 21, 193–204, https://doi.org/10.3208/sandf1972.21.2_1, 1981.

Casagli, N., Rinaldi, M., Gargini, A., and Curini, A.: Pore water pressure and streambank stability: results from a monitoring site on the Sieve River (Italy). Earth Surf. Proc. Land., 24, 1095–1114, https://doi.org/10.1002/(SICI)1096-9837(199911)24:12<1095::AID-ESP37>3.0.CO;2-F, 1999.

Chen, C. H., Hsieh, T. Y., and Yang, J. C.: Investigating effect of water level variation and surface tension crack on riverbank stability, J. Hydro-Environ. Res., 15, 41-53, https://doi.org/10.1016/j.jher.2017.02.002, 2017.

Chen, D. and Duan, J. G.: Modeling width adjustment in meandering channels, J. Hydrol., 321, 59–76, https://doi.org/10.1016/j.jhydrol.2005.07.034, 2006.

https://doi.org/10.5194/esurf-2021-97
Preprint. Discussion started: 20 December 2021

Chiang, S.W., Tsai, T.L., and Yang, J.C.: Conjunction effect of stream water stage and groundwater flow for riverbank stability analysis, Environ. Earth Sci., 62, 707–715, https://doi.org/10.1007/s12665-010-0557-8, 2011.

Clark, L. A. and Wynn, T. M.: Methods for determining streambank critical shear stress and soil erodibility: Implications for erosion rate predictions, T. ASABE, 50, 95–106, https://doi.org/10.13031/2013.19885, 2007.

Dapporto, S., Rinaldi, M., and Casagli, N.: Mechanisms of failure and pore water pressure conditions: Analysis of a riverbank along the ArnoRiver (central Italy), Eng. Geol., 61, 221– 242, https://doi.org/10.1016/S0013-7952(01)00026-6, 2001.

Darby, S. E., Alabyan, A. M., and Van de Wiel, M. J.: Numerical simulation of bank erosion and channel migration in meandering rivers, Water Resour. Res., 38, 1163, https://doi.org/10.1029/2001WR000602, 2002.

Darby, S. E., Rinaldi, M., and Dapporto, S.: Coupled simulations of fluvial erosion and mass wasting for cohesive river banks, J. Geophys-Earth., 112, F03022, https://doi.org/10.1029/2006JF000722, 2007.

Darby, S. E., Gessler, D., and Thorne, C. R.: Computer program for stability analysis of steep, cohesive riverbanks, Earth Surf. Proc. Land., 25, 175-190, https://doi.org/10.1002/(SICI)1096-9837(200002)25:2<175::AID-ESP74>3.3.CO;2-B, 2000.

Duan, G., Shu, A., Matteo, R., Wang, S., and Zhu, F.: Collapsing mechanisms of the typical cohesive riverbank along the Ningxia-Inner Mongolia catchment, Water, 9, 1272, https://doi.org/10.3390/w10091272, 2018.

Deng, S., Xia, J., and Zhou, M.: Coupled two-dimensional modeling of bed evolution and bank erosion in the Upper JingJiang Reach of Middle Yangtze River, Geomorphology, 344, 10-24, https://doi.org/10.1016/j.geomorph.2019.07.010, 2019.

Deng, S., Xia, J., Zhou, M., and Lin, F.: Coupled modeling of bed deformation and bank erosion in Jingjiang Reach of the Middle Yangtze River, J. Hydrol., 568, 221-233, https://doi.org/10.1016/j.jhydrol.2018.10.065, 2019.

Hackney, C., Best, J., Leyland, J., Darby, S. E., Parsons, D., and Aalto, R.: Modulation of outer bank erosion by slump blocks: disentangling the protective and destructive role of failed material on the three-dimensional flow structures, Geophy. Res. Lett., 42, 10663-10670, https://doi.org/10.1002/2015GL066481, 2015.

Hooke, J. M.: Magnitude and distribution of rates of river bank erosion, Earth Surf. Proc. Land., 5, 143– 157, https://doi.org/10.1002/esp.3760050205, 1980.

Huang, C., Gong, M., Qian, W., and Zhao, X.: Review of the study on the energy balance in sediment-laden flow, *J.* Water Resour. Eng., 16, 10-14. https://doi.org/10.3969/j.issn.1672-643X.2005.01.002, 2005.

Jia, D., Shao, X., Wang, H., and Zhou, G.: Three-dimensional modeling of bank erosion and morphological changes in the Shishou bend of the middle Yangtze River, Adv. Water Resour., 3, 348–360, https://doi.org/10.1016/j.advwatres.2010.01.002, 2010.

Langendoen, E. J. and Simon, A.: Modeling the evolution of incised streams. II: Streambank erosion, J. Hydraul. Eng., 134, 905–915. https://doi.org/10.1061/(ASCE)0733-9429(2008)134:7(905), 2008.

Lawler, D. M., Bull, L., and Harris, N. M.: Bank erosion events and processes in the Upper Severn, Hydrol. Earth Syst. Sc., 1, 523– 534, https://doi.org/10.5194/hess-1-523-1997, 1997.

Lopez Dubon, S. and Lanzoni, S.: Meandering evolution and width variations: A physics-statistics-based modeling approach, Water Resour. Res., 55, 76-94, https://doi.org/10.1029/2018WR023639, 2019.

Masoodi, A., Majdzadeh Tabatabai, M. R., Noorzad, A., and Samadi, A.: Effects of soil physico-chemical properties on stream bank erosion induced by seepage in northeastern Iran, Hydrolog. Sci. J., 62, 2597-2613. https://doi.org/10.1080/02626667.2017.1403030, 2017.

Masoodi, A., Majdzadeh Tabatabai, M. R., Noorzad, A., and Samadi, A.: Riverbank stability under the influence of soil dispersion phenomenon, J. Hydraul. Eng., 24, 5019001., https://doi.org/10.1061/(ASCE)HE.1943-5584.0001756, 2019.

Motta, D., Abad, J. D., Langendoen, E. J., and Garcia, M. H.: A simplified 2D model for meander migration with physically-based bank evolution, Geomorphology, 163, 10–25, https://doi.org/10.1016/j.geomorph.2011.06.036, 2012.

https://doi.org/10.5194/esurf-2021-97
Preprint. Discussion started: 20 December 2021

Motta, D., Langendoen, E. J., Abad, J. D., and García, M. H.: Modification of meander migration by bank failures, J. Geophys. Res-Earth., 119, 1026–1042, https://doi.org/10.1002/2013JF002952, 2014.

Nagata, N., Hosoda, T., and Muramoto, Y.: Numerical Analysis of River Channel Processes with Bank Erosion, J. Hydraul. Eng., 4, 243–252, https://doi.org/10.1061/(ASCE)0733-9429(2000)126:4(243), 2000.

Osman, A. M. and Thorne, C. R.: Riverbank Stability Analysis. I: Theory, J. Hydraul. Eng., 114, 134-150, https://doi.org/10.1061/(ASCE)0733-9429(1988)114:2(134), 1988.

Parker, C., Simon, A., and Thorne, C. R.: The effects of variability in bank material properties on riverbank stability: Goodwin Creek, Mississippi, Geomorphology, 101, 533–543, https://doi.org/10.1016/j.geomorph.2008.02.007, 2008.

Patsinghasanee, S., Kimura, I., Shimizu, Y., Nabi, M., and Chub-Uppakarn, T.: Coupled studies of fluvial erosion and cantilever failure for cohesive riverbanks: Case studies in the experimental flumes and U-Tapao River, J. Hydro-Environ. Res., 16, 13-26, https://doi.org/10.1016/j.jher.2017.04.002, 2017.

Qian, N., Wan, Z., and Yang, J. (Eds): Sediment motion mechanics, Science Press, Beijing, ISBN: 9787030112606, 1983.

Qian, N. and Wan, Z.: A preliminary study on the influence of near-bottom high sediment concentration layer on water flow and sediment movement, J. Hydraul. Eng., 4, 3-22, https://doi.org/CNKI: SUN: SLXB.0.1965-04-000, 1965.

Rijn, V. and Leo, C.: Sediment Transport, Part I: Bed Load Transport, J. Hydraul. Eng., 110,1431-1456, https://doi.org/10.1061/(ASCE)0733-9429(1984)110:10(1431), 1985.

Rinaldi, M., Casagli, N., Dapporto, S., and Gargini, A.: Monitoring and modelling of pore water pressure changes and riverbank stability during flow events, Earth Surf. Proc. Land., 29, 237–254, https://doi.org/10.1002/esp.1042, 2004.

Rinaldi, M., Mengoni, B., Luppi, L., Darby, S. E., and Mosselman, E.: Numerical simulation of hydrodynamics and bank erosion in a river bend. Water Resource Research, 44, W09428, https://doi.org/10.1029/2008WR007008, 2008.

Rinaldi, M. and Nardi, L.: Modeling Interactions between Riverbank Hydrology and Mass Failures, J. Hydraul. Eng., 18, 1231-1240, https://doi.org/10.1061/(ASCE)HE.1943-5584.0000716, 2013.

Shu, A., Duan, G., Rubinato, M., Tian, L., Wang, M., and Wang, S.: An Experimental Study on Mechanisms for Sediment Transformation Due to Riverbank Collapse, Water, 11, 529, https://doi.org/10.3390/w11030529, 2019.

Shu, A., Liu, Q., Yi Y., and Zhang Z.: Characteristics of energy dissipation in hyperconcentrated flows, Int. J. Sediment Res., 23, 387–397, https://doi.org/10.1016/s1001-6279(09)60009-3, 2008.

Shu, A., Zhang, K., and Fei, X.: Transfer and dissipation laws of turbulent energy in hyper concentrated flow, J. Hydraul. Eng., 38, 383-388, https://doi.org/10.3321/j.issn:0559-9350.2007.04.001, 2007.

Simon, A. and Collison, A. J. C.: Quantifying the mechanical and hydrologic effects of riparian vegetation on streambank stability, Earth Surf. Proc. Land., 27, 527-546, https://doi.org/10.1002/esp.325, 2002.

Simon, A., Curini, A., Darby, S. E., and Langendoen, E. J.: Bank and near-bank processes in an incised channel, Geomorphology, 35, 193-217, https://doi.org/10.1016/s0169-555x(00)00036-2, 2000.

Simon, A. and Rinaldi, M.: Disturbance, stream incision, and channel evolution: The roles of excess transport capacity and boundary materials in controlling channel response, Geomorphology, 79, 361–383, https://doi.org/10.1016/j.geomorph.2006.06.037, 2006.

Simon, A., Pollen-Bankhead, N., Mahacek, V., and Langendoen, E. J.: Quantifying reductions of mass-failure frequency and sediment loadings from streambanks using toe protection, *J. Am. Water Resour. As.*, 45, 170-186, https://doi.org/10.1111/j.1752-1688.2008.00268.x, 2009.

Thorne, C. R. and Tovey, N. K.: Stability of composite river banks, Earth Surf. Proc. Land., 6, 469–484, https://doi.org/10.1002/esp.3290060507, 1981.

Visconti, F., Camporeale, C., and Ridolfi, L.: Role of discharge variability on pseudomeandering channel morphodynamics: Results from laboratory experiments, J. Geophys. Res-Earth., 115, F04042, https://doi.org/10.1029/2010JF001742, 2010.

https://doi.org/10.5194/esurf-2021-97
Preprint. Discussion started: 20 December 2021

Wood, A., Simon, A., Downs, P. W., and Thorne, C. R., Bank-toe processes in incised channels: The role of apparent cohesion in the entrainment of failed bank materials, Hydrol. Process., 15, 39–61, https://doi.org/10.1002/hyp.151, 2001.

Xia, J., Deng, S., Lu J., Xu, Q., Zong, Q., and Tan, G.: Dynamic channel adjustments in the Jingjiang Reach of the Middle Yangtze River, Sci. Rep-UK, 6, 22802, https://doi.org/10.1038/srep22802, 2016.

Xu, D., Bai, Y., Ma, J., and Tan, Y.: Numerical investigation of long-term planform dynamics and stability of river meandering on fluvial floodplains, Geomorphology, 132, 195–207, https://doi.org/10.1016/j.geomorph.2011.05.009, 2011.

Yu, G., Li, Z., Yang, H., Lu, J., Huang, H., and Yi, Y.: Effects of riparian plant roots on the unconsolidated bank stability of meandering channels in the Tarim River, China, Geomorphology, 351,106958, https://doi.org/10.1016/j.geomorph.2019.106958., 2020.

Yu, M., Chen, X., Wei, H., Hu, C., and Wu, S.: Experiment of the influence of different near-bank riverbed compositions on bank failure, Adv. Water Sci., 2, 176–185, https://doi.org/10.14042/j.cnki.32.1309.2016.02.002, 2016.

Yu, M. and Guo, X.: Experimental study on the interaction between the hydraulic transport of failed bank soil and near-bank bed evolution, Adv. Water Sci., 5, 677–683, https://doi.org/10.14264/uql.2014.317, 2014.

Yu, M., Shen, K, Wu, S, and Wei, H.: An experimental study of interaction between bank collapse and riverbed evolution. Adv. Water Sci., 5, 675–682, https://doi.org/10.14042/j.cnki.32.1309.2013.05.001, 2013.

Zhang, R.: A review on the gravitation theory of sediment suspension, J. Hydraul. Eng., 3, 11-23, https://doi.org/CNKI:SUN:SLXB.0.1963-03-001, 1963.

Zhao, K., Gong, Z., Xu, F., Zhou, Z., Zhang, C., Perillo, G., and Coco, G.: The role of collapsed bank soil on tidal channel evolution: A process-based model involving bank collapse and sediment dynamics, Water Resour. Res., 55, 9051-9071, https://doi.org/10.1029/2019WR025514, 2019.